Optimal component location for PI observer based active control of a galvanizing process.

Mohammed Brakna [*,**] **Benoît Marx** [*] **Van Thang Pham** [**]
Ahmed Khelassi [**] **Didier Maquin** [*] **José Ragot** [*]

[*] *Université de Lorraine, CNRS, CRAN, BP 70239, 54506 Vandœuvre-lès-Nancy, France (e-mail: {mohammed.brakna, benoit.marx, didier.maquin, jose.ragot}@univ-lorraine.fr).*
[**] *ArcelorMittal Maizières Research SA, BP 30320. Voie Romaine, 57283 Maizières-lès-Metz, France (e-mail: {vanthang.pham, ahmed.khelassi}@arcelormittal.com)*

Abstract: Optimal sensor and actuator placement is performed for active vibration control. The components are selected to minimize the vibration impact on the strip by $\mathcal{H}_2$-norm minimization. Then, active vibration control is based on a PI-observer design allowing, not only to estimate the state, but also the disturbances. Some numerical results illustrate the performance of the proposed active vibration control.

Keywords: Optimal actuator placement, optimal sensor placement, PI-observer-based control, perturbation reduction, galvanizing process.

1. INTRODUCTION

Reducing vibrations on a galvanizing line will improve efficiency by minimizing maintenance costs and energy consumption. To do so, optimal placement of sensors and actuators can be the solution, allowing to maximize both the information collected on the process and the efficiency of the active vibration control.
Based on optimization notions and control theory, the choice of component placement is used in different industrial fields as water network and treatment (Villez et al., 2016), steel industry (Wang et al., 2016), vibration control (Botta et al., 2013). Several methods exist to reduce/reject the disturbance such as a model based-control method using a feedforward control in Saxinger et al. (2020). These methods can be divided into heuristic-based approach (e.g. TABOU technique (Kincaid and Padula, 2002)) and analytical approach (e.g. H_2 optimization).

An overview of the optimal placement of sensors and actuators for active vibration control of flexible structures is presented in (Borairi and Soufian, 2017), two algebraic Riccati equations are formulated for the control and the observation. A relation between sensor placement, fault detection and isolation is shown in (Rostek, 2015), where a branch-and-bound algorithm is used to solve the integer optimization problem. In this paper, the simultaneous placement of sensors and actuators method is addressed. Different approaches can be cited as Gramian-based method for linear time-invariant descriptor systems (Marx et al., 2004). In (Dhingra et al., 2014) the solution of optimal components placement is proposed via linear convex relaxation method using the so-called alternating direction method of multipliers. The $\mathcal{H}_2/\mathcal{H}_\infty$ strategy is used in (Deshpande and Bhattacharya, 2021) for observer design, without any control objectives. The same strategy with $\mathcal{D}$-stability for dynamic output feedback control is applied in (Argha et al., 2016) but conduct to large LMI problems and thus to numerical problems. In (Brakna et al., 2021) the optimal placement of sensors and actuators is obtained by minimizing the energy transfer from disturbances to the controlled output using $\mathcal{H}_2$ strategy but the disturbance estimation was not envisaged.

The present paper is divided into fourth steps. The first step, detailed in the second section, consists in the development of a vibration propagation model in the steel strip using the partial differential equation (PDE) describing an axially moving strip. The third section is devoted to the

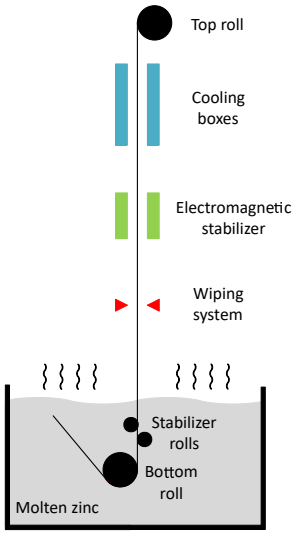

Fig. 1. Schematic diagram of the galvanizing process

principal problem: the search for the optimal placement of the sensors and actuators to minimize the disturbance effect on the behavior of the steel strip. In section four, are gathered the simulation results of the active vibration control based on the optimal placement of sensors and actuators, and finally some remarks are given.

2. STRIP MODELING

The continuous hot-dip galvanizing process could be modeled as an axially moving strip steel. The interesting part of the strip is between the top and the stabilizing rolls (see Figure 1) of uniform volumic mass ρ, damping coefficient c and a thickness of h pulled by a specific tension N_ξ and traveling at a velocity of v. The strip is excited by a force $F(\zeta,\xi,t)$ including disturbances from the air-knife of the wiping system and cooling boxes, and/or electromagnets force, ζ,ξ are the vertical and horizontal position (see Figure 1). The transversal displacement $z(\zeta,\xi,t)$ is deduced from the solution of the following partial differential equation (PDE):

$$\begin{aligned} D\nabla^{(4)}z + \rho h(\frac{\partial^2 z}{\partial t^2} + 2v\frac{\partial^2 z}{\partial\zeta\partial t} + v^2\frac{\partial^2 z}{\partial\zeta^2}) - N_\xi\frac{\partial^2 z}{\partial\zeta^2} \\ + c(\frac{\partial z}{\partial t} + v\frac{\partial z}{\partial\zeta}) = F(\zeta,\xi,t) \end{aligned} \quad (1)$$

where

$$\nabla^{(4)} = \frac{\partial^4}{\partial\zeta^4} + 2\frac{\partial^4}{\partial\zeta^2\partial\xi^2} + \frac{\partial^4}{\partial\xi^4}, D = \frac{Eh^3}{12(1-\nu)}$$

and D, E, ν are respectively the flexural rigidity, Young's modulus and Poisson coefficient.

Remark 1. The pilot used for the tests has a length of $L_\zeta = 7.2m$ between the two rolls and a width of $L_\xi = 1.2m$.

2.1 Numerical solution of the PDE

The method used to solve (1) consists in discretizing the spatial variables (ζ,ξ) by the finite difference method using differential quotients based on the Taylor series expansions in order to transform a PDE into an ordinary differential equation ODE. The equation (1) becomes:

$$\begin{aligned} \ddot{z}_{i,j} &= b_1\dot{z}_{i,j} + b_2\dot{z}_{i+1,j} + b_3\dot{z}_{i-1,j} + a_1 z_{i,j} + a_2 z_{i+1,j} \\ &+ a_3 z_{i-1,j} + a_4(z_{i,j+1} + z_{i,j-1}) + a_5(z_{i+2,j} + z_{i-2,j}) \\ &+ a_6(z_{i,j+2} + z_{i,j-2}) + a_7(z_{i+1,j+1} + z_{i+1,j-1} \\ &+ z_{i-1,j+1} + z_{i-1,j-1}) + a_8(u_{i,j} + w_{i,j}) \end{aligned} \quad (2)$$

where the index $i \in \{1,..,N\}$ (resp. $j \in \{1,..,M\}$) denotes the vertical (resp. horizontal) position of the considered discretization points and N (resp. M) the number of the discretization points on the vertical (resp. horizontal) axis. The equations (2) of the system completed by the output matrix can be written as:

$$\begin{cases} \dot{x}(t) = Ax(t) + B_u u(t) + B_w w(t) \\ y(t) = Cx(t) \end{cases} \quad (3)$$

with $x = [z^T \dot{z}^T]^T$, where $z \in \mathbb{R}^n$ gathers the strip displacements at all discretized points, $w = [w_1, w_2, ...]^T \in \mathbb{R}^{n_w}$, $u \in \mathbb{R}^{n_p}$, A, B_u, B_w, C are the state, the control input, the disturbance and the output matrices.

2.2 Boundary conditions

As part of the solution of (1), the boundary conditions can be:

- Clamped and simply supported edges:
  - at the bottom: $z(0,\xi,t) = w_1(t), \forall\xi \in [0, L_\xi]$
  - at the top: $z(L_\zeta,\xi,t) = w_2(t), \forall\xi \in [0, L_\xi]$.
- Free edges:

$$\frac{\partial^2 z(\zeta,\xi,t)}{\partial\zeta^2} + \nu\frac{\partial^2 z(\zeta,\xi,t)}{\partial\xi^2} = 0 \quad \text{for } \xi = 0 \text{ and } \xi = L_\xi$$

2.3 Experimental modeling validation

The objective of this section is to validate the theoretical model developed in section 2.1. To do so, a comparison is made between the numerical simulation of (3) and the experimental data of the pilot equipped with an actuator and 3 sensors $S1, S2$ and $S3$ (as displayed on Figure 2).

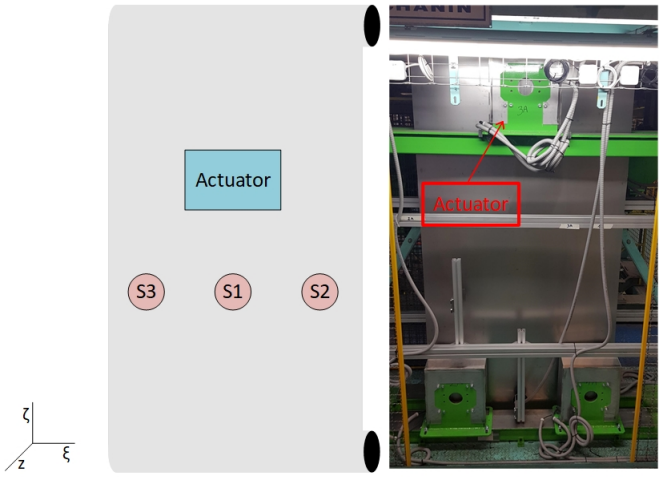

Fig. 2. The experimental pilot of the galvanizing line with the placement of sensors and actuators used for modeling validation.

The parameters and placement of the used components are defined in Table 1.

Table 1. Pilot parameters

Thickness	h	0.7 mm
Specific tension	N_ξ	17000 N/m
Volumic mass	ρ	7850 kg/m^3
Young's modulus	E	200 GPa
Damping	c	1
Actuator position	$\{\zeta,\xi\}_{act}$	$\{3.9, 0.6\}m$
Sensor position 1	$\{\zeta,\xi\}_{S_1}$	$\{3.2, 0.6\}m$
Sensor position 2	$\{\zeta,\xi\}_{S_2}$	$\{3.2, 0.2\}m$
Sensor position 3	$\{\zeta,\xi\}_{S_3}$	$\{3.2, 1.0\}m$

On Figure 3, one may compare the frequency contents of the free responses measured on the experimental pilot (blue lines) to the one simulated (red lines) with the model (2) augmented by an actuator model. The same input signal is applied on the pilot by an electromagnet actuator and on the simulator.

Remark 2. A similarity is observed in the free responses of the theoretical model and of the pilot on different locations

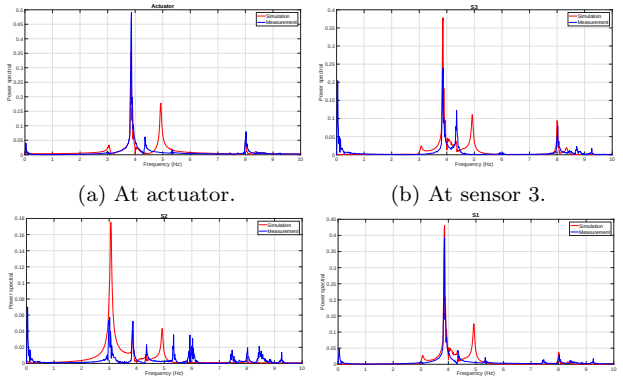

(a) At actuator. (b) At sensor 3.

(c) At sensor 2. (d) At sensor 1.

Fig. 3. Frequency responses around the first resonance frequency of the simulated (red) and measured (blue) free responses at different locations.

except for one of the free edges (the one equipped with the sensor $S2$). This discrepancy is caused by a slight asymmetry in the steel strip generating a non constant specific tension. The results in the Figure 3 illustrate the accuracy of the discretized model (2).

3. SENSOR/ACTUATOR POSITIONING STRATEGY FOR DISTURBANCE EFFECT REDUCTION OF THE GALVANIZING SYSTEM

As stated in the preamble, the disturbance effect reduction resulting from the steel strip vibrations is important for the efficiency of a galvanizing process. Although the system has been engineered so that its functioning minimizes the vibration impact its by mechanical conception, the design of the control system remains crucial and contributes to the steel strip stabilization.

As mentioned before, the optimal positioning of the sensors aims at providing an optimal estimation of the system states and disturbance affecting the steel strip behavior. The optimal actuators locations allows an optimal reduction of vibrations on the system. The problems of sensors and actuators locations may be addressed simultaneously if degrees of freedom exist in both placements.

In addition to the requirements previously cited, on the one hand, hardware constraints could be added: e.g. limited number of components for economic reasons or the prohibition of some component placements on the galvanizing line due to some technical or physical reasons. On the other hand, the software constraints are related to the state space dimension of the system because the capacities of the computer are limited for large calculations of the observer and the controller (e.g. even if the observer-based control is calculated off-line, the real time implementation needs also sufficient CPU capacity). In what follows, some of these constraints will not be taken into account, to focus on the optimal component placement for PIO-control based control.

Let us consider a large scale system with n state variables and p_n (resp. q_n) actuators (resp. sensors) to be placed, the number of possible configurations is $C_n^{n_p} \cdot C_n^{n_q}$. Furthermore, taking into account some physical or economical constraints limits the computational burden by defining a new set of possible placements for the actuators (resp. sensors) denoted $\mathcal{D}_a$ (resp. $\mathcal{D}_s$), defined by:

$$\begin{aligned} \mathcal{D}_a &= \{i \mid z_i \text{ can be actuated}\}, \\ \mathcal{D}_s &= \{j \mid z_j \text{ can be measured}\}, \end{aligned} \tag{4}$$

of cardinal $\tilde{p}$ (resp. $\tilde{q}$). The number of possible placements becomes : $C_{\tilde{p}}^{n_p} \cdot C_{\tilde{q}}^{n_q} < C_n^{n_p} \cdot C_n^{n_q}$. The considered dynamic system with a control u, output y and subject to a disturbance w, defined by $B_u(p) \in \mathbb{R}^{n \times n_p}$, $C(q) \in \mathbb{R}^{n_q \times n}$ and $B_w \in \mathbb{R}^{n \times n_w}$ respectively :

$$\begin{cases} \dot{x}(t) &= A\,x(t) + B_u(p)\,u(t) + B_w\,w(t) \\ y(t) &= C(q)\,x(t) \end{cases} \tag{5}$$

The system (5) includes two parameters $p \in \mathbb{N}^{n_p}$ and $q \in \mathbb{N}^{n_q}$ that can be defined as two vectors of integers whose entries are the number of the columns of B_u and of the rows of C in the system (3), corresponding to the selected actuators and sensors. These two parameters must be optimally chosen by placing the actuator and the sensor (resp. parameter p and q) in order to minimize the disturbance effect w on the system output y.

Remark 3. In order to optimize the computational cost, the author in Potami (2008) proposes to reduce the number of simultaneous optimal placement possibilities of components by imposing a collocation of the sensor/actuator couple ($p = q$). For the sake of generality, this hypothesis is not assumed in the presented results.

3.1 Observed state feedback control law

In order to efficiently control the perturbed system, an extended state feedback control law based on a PI observer is considered. The basic idea of this control configuration is to not only take benefits of the system state estimation for the control, but also to obtain an accurate estimation of the disturbance for process monitoring. To do so, a PI observer is used since it is well known for its ability to estimate unknown inputs (see Marx et al. (2003); Koenig and Mammar (2002)). The proportional integral observer is described by:

$$\begin{cases} \dot{\hat{x}}(t) &= A\hat{x}(t) + B_u(p)u(t) + B_w\hat{w}(t) + \\ & \quad L_y(q)(y(t) - \hat{y}(t)) \\ \hat{y}(t) &= C(q)\hat{x}(t) \\ \dot{\hat{w}}(t) &= L_w(q)(y(t) - \hat{y}(t)) \end{cases} \tag{6}$$

From (5) and (6), the state estimation error $e(t) = x(t) - \hat{x}(t)$ and the disturbance estimation error $e_w(t) = w(t) - \hat{w}(t)$ are described by:

$$\begin{cases} \dot{e}(t) = (A - L_y(q)C(q))e(t) + B_w e_w(t) \\ \dot{e}_w(t) = \dot{w}(t) - L_w(q)C(q)e(t) \end{cases} \tag{7}$$

where $L_y(q), L_w(q)$ are the gains of the PI observer (proportional and integral gains resp.). In matrix form it becomes :

$$\begin{bmatrix} \dot{e}(t) \\ \dot{e}_w(t) \end{bmatrix} = \left(\underbrace{\begin{bmatrix} A & B_w \\ 0 & 0 \end{bmatrix}}_{A_o} - \underbrace{\begin{bmatrix} L_y(q) \\ L_w(q) \end{bmatrix}}_{L_o(q)} \underbrace{\begin{bmatrix} C(q) & 0 \end{bmatrix}}_{C_o(q)} \right) \begin{bmatrix} e(t) \\ e_w(t) \end{bmatrix} \tag{8}$$

where $\dot{w}(t) = 0$ is assumed, which is a classical assumption when designing PI observer. The applied control law is defined by:

$$u(t) = -K_x(p)\hat{x}(t) - K_w(p)\hat{w}(t) \tag{9}$$

The closed-loop system (5)-(6)-(9) is:

$$\begin{cases} \dot{x}(t) = (A - B_u(p)K_x(p))x(t) + B_u(p)K_x(p)e(t) \\ \quad + B_u(p)K_w(p)e_w(t) + (B_w - B_u(p)K_w(p))w(t) \\ y(t) = C(q)x(t) \end{cases} \tag{10}$$

From (8) and (10), the augmented form can be written as:

$$\begin{cases} \dot{x}_c(t) = A_c(p,q)\, x_c(t) + B_c(p)\, w(t) \\ y(t) = C_c(q)\, x_c(t) \end{cases} \tag{11}$$

with $x_c(t) = \left[x^T(t)\ e^T(t)\ e_w^T(t)\right]^T$, $C_c(q) = [C(q)\ 0\ 0]$, $B_c(p) = [B_w - B_u(p)K_w(p)\ 0\ 0]^T$ and

$$A_c(p,q) = \begin{bmatrix} A - B_u(p)K_x(p) & B_u(p)\,K_x(p) & B_u(p)\,K_w(p) \\ 0 & A - L_y(q)\,C(q) & B_w \\ 0 & L_w(q)\,C(q) & 0 \end{bmatrix}$$

From the separation principle, the gain $L_o(q)$ is determined to make the matrix $(A_o - L_o(q)C_o(q))$ Hurwitz. Thus, from (8), $P(q)$ and $L_o(q)$ must satisfy the following matrix inequalities:

$$\begin{cases} (A_o - L_o(q)C_o(q))^T P(q) + P(q)(A_o - L_o(q)C_o(q)) < 0, \\ P(q) > 0 \end{cases} \tag{12}$$

where $P(q)$ is a symmetric positive definite matrix. The system (12) can be rewritten as:

$$\begin{cases} A_o^T P(q) + P(q)A_o - C_o^T(q)Q^T(q) - Q(q)C_o(q)) < 0, \\ P(q) > 0 \end{cases} \tag{13}$$

with $L_o(q) = P^{-1}(q)Q(q)$.

Lemma 1. Let us denote $\lambda \in \mathbb{C}$ the eigenvalues of matrix $(A_o - L_o(q)C_o(q))$. In order to improve the temporal response, the error estimation eigenvalues are placed in a vertical band defined by $Re(\lambda) \in [-2\beta, -2\alpha]$ (see Chilali et al. (1999)), with $\alpha > 0$ and $\beta > 0$,

$$\begin{cases} H(q)^T + H(q) < -\alpha P(q), \\ H(q)^T + H(q) > -\beta P(q) \end{cases} \tag{14}$$

where $H(q) = P(q)A_o - Q(q)C_o(q)$.
The observed state denoted $\hat{x}$ is provided by (6) and the feedback gain $K(p)$ is given by:

$$K(p) = [K_x(p)\ K_w(p)] \tag{15}$$

where

$$\begin{aligned} K_x(p) &= M^{-1}B_u^T(p)P_k(p) \\ K_w(p) &= M^{-1}B_u^T(p)h_w(p) \end{aligned} \tag{16}$$

$P_k(p)$ is the solution of the following Riccati equation:

$$A^T P_k(p) + P_k(p)A - P_k(p)B_u(p)M^{-1}B_u^T(p)P_k(p) + R = 0 \tag{17}$$

and $h_w(p)$ is defined by:

$$h_w(p) = (P_k(p)B_u(p)M^{-1}B_u^T(p) - A^T)^{-1}P_k(p)B_w \tag{18}$$

derived from the minimization of the following quadratic cost function:

$$\Phi = \int_0^\infty x(t)^T Rx(t) + u(t)^T Mu(t)dt \tag{19}$$

where R and M are two parameters respectively set to pay a particular attention to the vibration reduction on some given points of the strip and to limit the control energy.

3.2 Optimal positioning of the sensor/actuator pair

The dynamics of the augmented state system is presented in (11), according to the objective of reducing the disturbance effect on the controlled outputs ($y \in \mathbb{R}^{n/2}$) of the system Even if p and q are chosen, then the controller and the observer gains (resp. $K(p)$, $L(q)$) should be calculated. To evaluate the efficiency of observer-based control in minimizing the perturbation impact on the displacement states, the $\mathcal{H}_2$ or $\mathcal{H}_\infty$-norms criterion is chosen (only $\mathcal{H}_2$-gain is addressed below to envisage the whole frequency domain, and not only the worst case). From (11), the transfer function reflecting this influence is:

$$T_{yw}(p,q,s) = \tilde{C}_c(sI - A_c(p,q))^{-1}\, B_c(p) \tag{20}$$

where $\tilde{C}_c = \left[C_{n/2}\ 0_{n/2,3n/2+n_w}\right]$ selects all the variables z. Clearly the choice of a sensor/actuator subset (via p and q) has an influence on the disturbance effect reduction.

According to the complexity of the analytical expression of the transfer function $T_{yw}(p,q,s)$ that depends on p and q, finding the sensor/actuator pair is based on a numerical procedure. Initially the H_2-norm of the transfer $T_{yw}(p,q,s)$ is calculated by:

$$\| T_{yw}(p,q) \|_2^2 = trace\left(B_c^T(p)\tilde{P}(p,q)B_c(p)\right) \tag{21}$$

where $\tilde{P}(p,q)$ is the solution of the following Lyapunov equation:

$$A_c(p,q)^T\tilde{P}(p,q) + \tilde{P}(p,q)A_c(p,q) + \tilde{C}_c^T\tilde{C}_c = 0 \tag{22}$$

The solution is obtained by minimizing (21) with respect to the possible values of p and q:

$$\{\hat{p}, \hat{q}\} = argmin_{p\in\mathcal{D}_a, q\in\mathcal{D}_s} \| T_{yw}(p,q) \|_2^2 \tag{23}$$

Algorithm (1) gathers the different steps of the proposed optimal sensor/actuator placement for PI observer-based control.

Algorithm 1 Sensor/actuator positionning

```
Set up the matrices A,B_u,C and B_w from (3)
Define the parameters R, M , α and β in (19) and (14)
for p ∈ N^{n_p} s.t. p_i ∈ D_a and p_i ≠ p_j for i ≠ j do
  for q ∈ N^{n_q} s.t. q_i ∈ D_s and q_i ≠ q_j for i ≠ j do
    Update the matrices B_u(p) and C(q)
    Compute the gain L_o(q) by solving the LMI's (14)
    Compute the gain K(p) by solving (16) and (17)
    Update the matrices A_c(p,q), B_c(p) and C_c(q) in (11)
    Solve (22) with respect to P̃(p,q)
    Compute the norm ‖ T_yw(p,q) ‖_2^2 (21)
  end for
end for
Determine the solution p̂, q̂ by solving (23).
```

4. NUMERICAL RESULTS AND DISCUSSION

This section includes two parts. First, the proposed results for optimal component placement are illustrated. According to the vibrations sources, two cases are studied:

- Case A : The bottom roll is excited (the M first columns of B_w).
- Case B : The top and the bottom rolls are excited (all columns of B_w).

The Figure 4 represents the value of the $\mathcal{H}_2$ norm of the system (20) according to the sensor locations for a given actuator position. Among the $N = 18$ possible locations, only four choices are displayed for the sake of clarity.

The optimal placement obtained for a single component in case A is defined by $\{p_{opt}, q_{opt}\}_A = \{1, 1\}$ (corresponding to $\{\zeta, \xi\} = \{0.4, 0.4\}m$) and for the case B the optimal location of two sensors and two actuators is at $\{p_{opt}, q_{opt}\}_B = \{\{1, 18\}, \{1, 18\}\}$ corresponding to $\{\zeta, \xi\} = \{\{0.4, 6.8\}, \{0.4, 6.8\}\}m$.

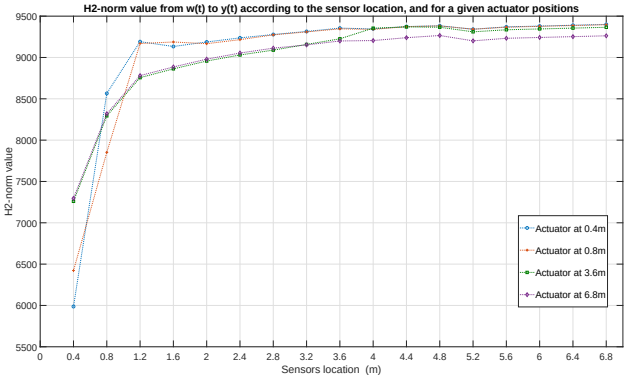

(a) Case A.

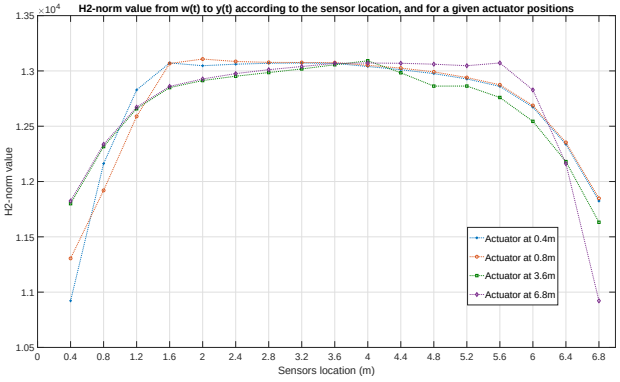

(b) Case B.

Fig. 4. $\mathcal{H}_2$ norm values of the system (20) according to the placement of the sensors and actuators.

Second, based on the obtained optimal sensor and actuator location, the PI observer and controller results are now presented. The state (resp. disturbance) estimation is illustrated on the Figure 5 (resp. 6).

As can be seen in the Figure 5, in the case A with one sensor placed at $\{\zeta, \xi\} = \{0.4, 0.4\}m$ in case A or in the case B with two sensors ($\{\zeta, \xi\} = \{\{0.4, 6.8\}, \{0.4, 6.8\}\}m$), all states of the system are correctly estimated. On the Figure 6, one can see that the disturbance affecting the steel strip is also accurately estimated.

In order to illustrate the efficiency of the proposed control, the open-loop and closed-loop strip behaviors are compared at different locations on the Figure 7.

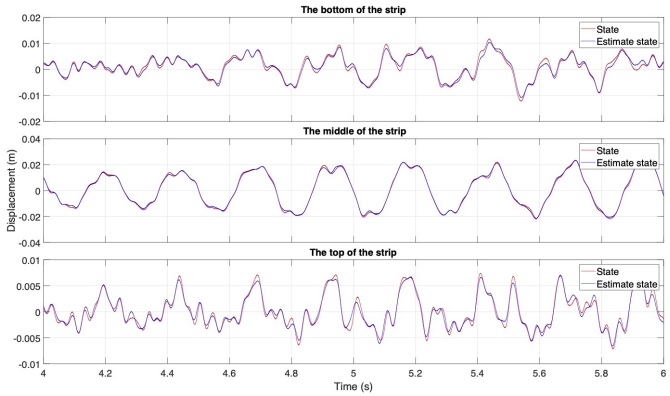

(a) Case A.

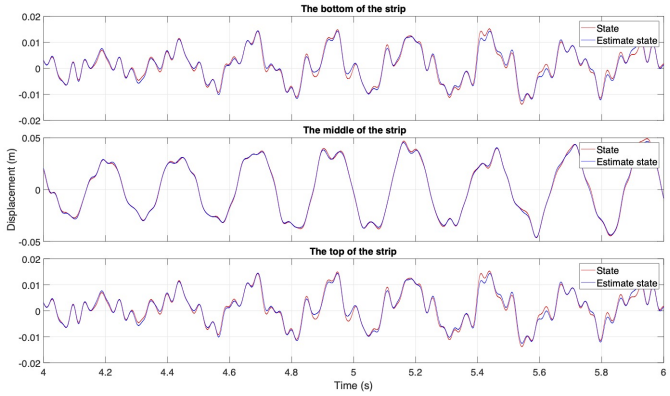

(b) Case B.

Fig. 5. Comparison between the system state and its estimate at the top, the middle and the bottom of the steel strip in the cases A and B.

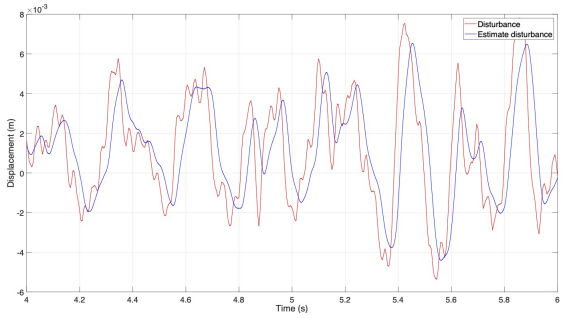

Fig. 6. Comparison between disturbance and its estimate.

Analyzing the Figure 7 and the data of the table 2, clearly the control based on the proposed optimal sensor and actuator location efficiently reduces the steel strip vibrations caused by the bottom (and top) roll(s) in both cases (in case A, the vibration amplitudes have been reduced six times in closed loop with the optimal placement, similar results are obtained for the case B). The energy in Table 2 is calculated by:

$$E = \sum_{i=0}^{N} \sum_{j=0}^{M} \sum_{k=0}^{T} (z(\zeta_i, \xi_j, t_k))^2$$

where T is the number of time instants.

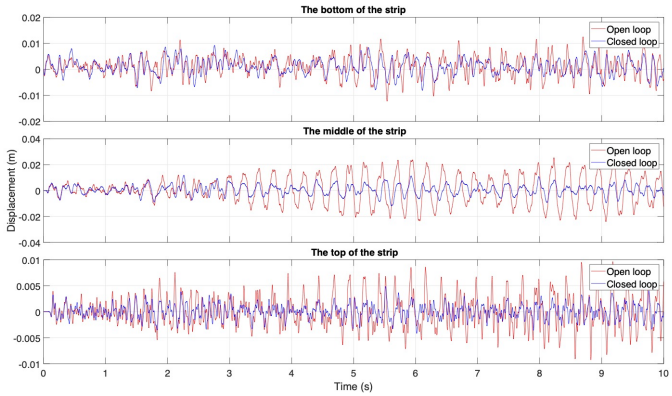

(a) Case A.

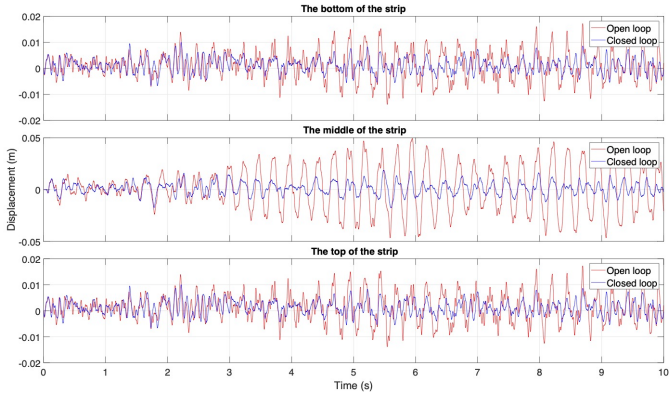

(b) Case B.

Fig. 7. Comparison of the system responses with and without active vibration control at different places of the steel strip (the top, the middle and the bottom) in the cases A and B.

Table 2: Energy of the system responses in open and closed-loop.

	Open-loop	Closed-loop	Closed-loop
optimal		No	Yes
$\{\zeta, \xi\}$	$\{\emptyset\}$	$\{4.0, 3.2\}m$	$\{0.4, 0.4\}m$
Case A	462.49	121.14	74.75

5. CONCLUSION AND PERSPECTIVE

The purpose of this paper is to find the optimal placement of actuators and sensors in order to reduce the disturbance impact on the behavior of the steel strip. this requires both the knowledge of the vibrations propagation model, closed-loop synthesis for the active control and the observer for the estimation of the system states. The proposed approach analyzes the efficiency of the sensor and actuator positioning to minimize the disturbances effect. The discretized model is validated by the results obtained during the experimental trials, simulations results of the closed-loop system with optimal sensor and actuator placement were performed and presented. The next works will be focused to the implementation of the current results of the active control on experimental pilot to validate the theoretical results and extend these results to improve the control system performances.

REFERENCES

Argha, A., Su, S.W., and Savkin, A. (2016). Optimal actuator/sensor selection through dynamic output feedback. In *2016 IEEE 55th Conference on Decision and Control (CDC)*, 3624–3629.

Borairi, M. and Soufian, M. (2017). Optimal actuator / sensor placement and controller design for large flexible space structures and robotics. In *IEEE International Symposium on Industrial Electronics*. Edinburgh, UK.

Botta, F., Dini, D., Schwingshackl, C., Di Mare, L., and Cerri, G. (2013). Optimal placement of piezoelectric plates to control multimode vibrations of a beam. *Advances in Acoustics and Vibration*, 2013, ID 905160.

Brakna, M., Marx, B., Pham, V., Khelassi, A., Maquin, D., and Ragot, J. (2021). Sensor and actuator optimal location for robust control of a galvanizing process. In *6th IFAC Workshop on Mining, Mineral and Metal Processing*. Nancy, FRANCE.

Chilali, M., Gahinet, P., and Apkarian, P. (1999). Robust pole placement in LMI regions. *IEEE Transactions on Automatic Control*, 44(12), 2257–2270.

Deshpande, V.M. and Bhattacharya, R. (2021). Sparse sensing and optimal precision: An integrated framework for $\mathcal{H}_2/\mathcal{H}_\infty$ optimal observer design. *IEEE Control Systems Letters*, 5(2), 481–486.

Dhingra, N.K., Jovanovic, M.R., and Luo, Z. (2014). An ADMM (alternating direction method of multipliers) algorithm for optimal sensor and actuator selection. In *53rd IEEE Conference on Decision and Control*, 4039–4044. Los Angeles, CA, USA.

Kincaid, R.K. and Padula, S.L. (2002). D-optimal designs for sensor and actuator locations. *Computers and Operations Research*, 29(6), 701–713.

Koenig, D. and Mammar, S. (2002). Design of proportional-integral observer for unknown input descriptor systems. *IEEE Transactions on Automatic Control*, 47, 2057– 2062.

Marx, B., Koenig, D., and Georges, D. (2004). Optimal sensor and actuator location for descriptor systems using generalized Gramians and balanced realizations. In *American Control Conference*. Boston, MA, USA.

Marx, B., Koenig, D., and Georges, D. (2003). Robust fault diagnosis for linear descriptor systems using proportional integral observers. In *42nd IEEE Conference on Decision and Control*, volume 1, 457 – 462 Vol.1. Maui, USA.

Potami, R. (2008). *Optimal sensor/actuator placement and switching schemes for control of flexible structures*. Ph.D. thesis, Worcester Polytechnic Institute, MA,USA.

Rostek, K. (2015). *Advanced Mechatronics Solutions*, chapter Optimal Sensor Placement for Fault Information System. Springer.

Saxinger, M. Marko, L., Steinboeck, A., and Kugi, A. (2020). Feedforward control of the transverse strip profile in hot-dip galvanizing lines. *Journal of Process Control*, 92, 35–49.

Villez, K., Vanrolleghem, P., and Corominas, L. (2016). Optimal flow sensor placement on wastewater treatment plants. *Water Research*, 101, 75–83.

Wang, Y.Q., Huang, X.B., and Li, J. (2016). Hydroelastic dynamic analysis of axially moving plates in continuous hot-dip galvanizing process. *International Journal of Mechanical Sciences*, 110, 201–216.